

Selenide glass single mode optical fiber for nonlinear optics

Houizot Patrick ^a, Smektala Frédéric ^{a,*}, Couderc Vincent ^b,
Troles Johann ^a, Grossard Ludovic ^b

^a UMR CNRS 6512 Verres et Céramiques, Bât 10B, Bureau 222, Université de Rennes 1, Campus de Beaulieu, 35042 Rennes Cedex, France

^b UMR CNRS 6615 Institut de Recherches en Communications Optiques et Micro-ondes, Faculté des Sciences, 123 av. A. Thomas, 87060 Limoges, France

Received 21 July 2005; accepted 24 November 2005

Available online 6 January 2006

Abstract

The physical characteristics, expansion coefficient, vitreous transition temperature and refractive index of several chalcogenide glasses based on the $\text{Ge}_x\text{Se}_{100-x}$ ($15 \leq x \leq 25$) system are studied. A couple of core/clad compositions is chosen with the purpose of the elaboration of single mode optical fibers. The fibers are obtained through a modified drawing process allowing to reduce the number of steps in the single mode fiberization procedure. The optical losses, the linear and nonlinear optical characterizations at 1.55 μm are presented. © 2005 Elsevier B.V. All rights reserved.

1. Introduction

The third order nonlinear optical properties of chalcogenide glasses are of great interest for the realization of nonlinear optical devices in the infrared. Raman amplification [1], supercontinuum generation [2], all optical switching and 3R regeneration are several examples of the optical functions that can be achieved with highly nonlinear materials [3–10]. Indeed, chalcogenide glasses combine a high intrinsic nonlinearity (100–1000 times the nonlinearity of silica glass depending on the composition) to a high transparency in the infrared (10–20 μm depending on the composition) [7,9,11–13]. These chalcogenide glasses can be synthesized from sulfur, selenium, tellurium or a combination of these elements in association with various other elements such as for example gallium, germanium, arsenic, antimony... Depending on the exact composition, we observe important variations in the physical properties: band gap and multiphonon edges, vitreous transition tem-

perature (T_g), expansion coefficient (α) and refractive index (n).

In this work we focus on the GeSe system and more particularly on several compositions close to the nominal GeSe_4 one. This glass exhibits a nonlinearity around 400 times higher than that of silica glass as measured on a bulk sample by different techniques [11–17]. The transparency range is varying from 730 nm to 16 μm for the bulk. We present here the study of the elaboration of single mode optical fibers from this glass. The composition dependence of the physical parameters (α , T_g , n) is investigated. A modified drawing process allowing a reduction of the number of step in the fiberization procedure is described. The achievements in the single mode fibers elaboration and their linear and nonlinear optical characterizations are presented.

2. Experimental procedure

2.1. Glass synthesis and physical characterizations

For the glass preparation we use high purity germanium and selenium elements (5 N). The selenium is further heated at 250 °C for several hours to eliminate surface oxide contamination by volatilization technique since its

* Corresponding author. Tel.: +33 2 23 23 56 20; fax: +33 2 23 23 56 11.
E-mail address: Frederic.Smektala@univ-rennes1.fr (S. Frédéric).
URL: www.verceram.univ-rennes1.fr (S. Frédéric).

oxides present greater vapor pressures than the element. The elements are put together and sealed in a silica tube under vacuum. The batch is heated at 850 °C in a rocking furnace and homogenized at this temperature during 12 h before the diminution of the temperature at 750 °C to partly condense the selenium vapors. Then the silica ampoule is quenched in water to obtain the glass, which is then annealed during 4 h near its glass transition temperature [11,12].

Different compositions based on the $\text{Ge}_x\text{Se}_{(100-x)}$ system with $15 \leq x \leq 25$ are studied to define core and clad glasses compatible with the drawing conditions. Thus, vitreous transition temperatures, expansion coefficients and refractive indices are measured. The thermal analyses are carried out on single glass chips in sealed aluminum pans. The measurements are performed with a Setaram 131 differential scanning calorimeter (DSC) from room temperature to 500 °C with a heating rate of 10 °C/min and allow the determination of the transition temperature of the glasses. The samples for the measurement of thermal expansion coefficients are cylinders with a diameter of 6 mm and a length of 15 mm. The two ends of the samples are polished to obtain two parallel faces. The heating rate is 3 °C/min. The measurements of the refractive index at 1.55 μm are realized with a Metricon 2010 prism coupler refractometer on cylindrical samples of 2 mm length and with two parallel faces.

2.2. Drawing process

2.2.1. Preform elaboration

The preform elaboration is based on the rod in tube method [18], which consists to insert a rod with core glass composition in a clad composition tube. Here, instead the utilization of a classic core rod of about 4 mm in diameter, we place in the cladding tube a core fiber which diameter is 400 μm (Fig. 1). The cladding tube is made by the rotational casting method [19]. The molten clad glass contained in a quartz ampoule is put in fast horizontal rotation, between 3000 round/min and 5000 round/min and cooled

to solidify the glass in a tube shape. The dimensions are typically 4 mm for internal diameter and 12 mm for external diameter.

The core fiber is then held in the center of the clad tube by the help of a PTFE crosspiece (Fig. 1). The clad tube is put together with a stainless steel tube by the help of a silica tube. The metallic tube is fixed to the vertical translation system of the drawing tower. This assembly allows to create a vacuum at the interface between the core fiber and the clad tube during the drawing to fill the space between the fiber and the tube. The vacuum is produced by a vacuum pump connected to the drawing tower by the metallic tube.

The aim of the process is to achieve the single mode fiber parameters (i.e. a core diameter of 10 μm) with a reduced number of steps: the clad tube fabrication, the 400 μm core fiber drawing and the final fiber-in-tube fiber drawing.

2.2.2. Fiber elaboration

After the elaboration of the “fiber-in-tube” preform and its fixing on the drawing tower, the preform is heated to 380 °C with a heating rate of 10 °C/min to reach a viscosity compatible with the formation of a drop. The drop which comes down under the gravity effect allows to draw the preform and to realize the beginning of the fiber. Then, this fiber is fixed on the rolling up drum whose speed rotation permit to control the diameter of the fiber. When the fiber is fixed on the drum, we create a vacuum at the interface between the core fiber and the tube to collapse the clad tube on the core fiber. Thus, the double index fiber with a small core corresponding to a single mode guiding configuration is realized in only one final drawing of the “fiber-in-tube” perform (Fig. 2).

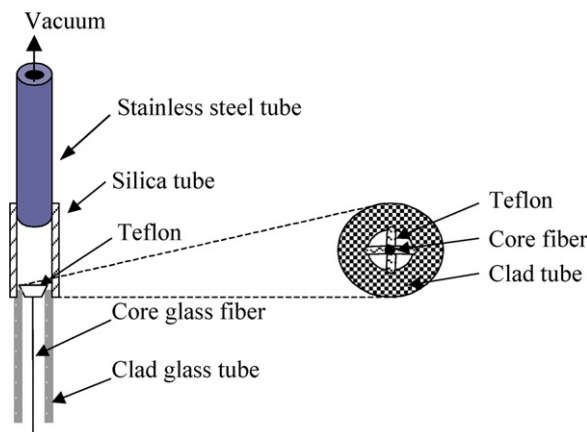


Fig. 1. Fiber-in-tube assembling.

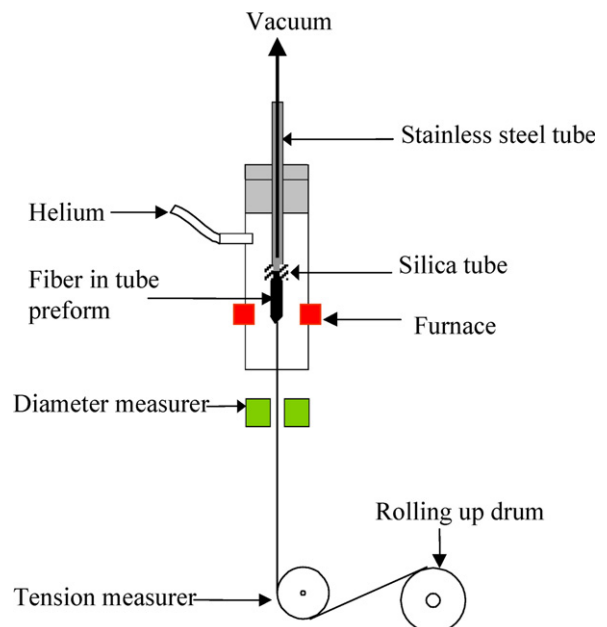


Fig. 2. Fiber-in-tube drawing.

2.3. Single mode optical fibers

2.3.1. Linear characterizations

The attenuation measurements at 1.55 μm are realized by the cut back technique [20], thanks to a laser diode emitting at this wavelength with a power of 3 mW. The detector is a photodiode InGaAs with an area of detection of 1 mm^2 .

To analyze the single mode character of the fiber, an erbium fiber laser single mode at 1.55 μm is used for the injection. A CCD-IR camera allows the detection. Then, a SPIRICON software analyzes the profile of the guided beam.

2.3.2. Nonlinear optical characterizations

The self phase modulation method is used for the determination of the nonlinear coefficient of the fiber. The injection in the single mode chalcogenide fiber is realized with an erbium fiber laser single mode at 1.55 μm . A photodetector coupled to an oscilloscope is used to detect the signal. The spectral broadening of the injected beam as a function of the peak power is measured at -20 dB. The nonlinear refractive index (n_2) is determined through a software of a program which calculates the temporal profile of a pulse during its propagation in an optical fiber presenting a third order nonlinearity, using the split-step Fourier method [21].

3. Experimental results

3.1. Physical characteristics

We have measured the vitreous transition temperatures for different compositions of the $\text{Ge}_x\text{Se}_{100-x}$ system with $15 \leq x \leq 25$. The results presented in Fig. 3 show the evolution of the T_g and the expansion coefficient when the germanium rate increases. The T_g increases highly with the germanium content. An augmentation of about 1% of Ge causes an augmentation of the T_g of about 4%. In the same way the expansion coefficient (α) of this vitreous system shows an important diminution when the germanium rate increases. The $\text{Ge}_{20}\text{Se}_{80}$ glass has an expansion coefficient

equal to $280 \times 10^{-7} \text{K}^{-1} \pm 5 \times 10^{-7} \text{K}^{-1}$ when it is equal to $230 \times 10^{-7} \text{K}^{-1} \pm 5 \times 10^{-7} \text{K}^{-1}$ for the $\text{Ge}_{25}\text{Se}_{75}$ glass. This represents an α variation of about 18% for a Ge content variation of 5%.

The measurements of the refractive index have been realized for $x = 18, 20, 21$ in $\text{Ge}_x\text{Se}_{100-x}$ system. The refractive indices are equal to $2.4493 \pm 5 \times 10^{-4}$, $2.4445 \pm 5 \times 10^{-4}$, and $2.4421 \pm 5 \times 10^{-4}$, respectively (Fig. 4).

These results allow the definition of a couple of glasses compatible with the elaboration of a single mode fiber. The $\text{Ge}_{20}\text{Se}_{80}$ glass is chosen as the core composition. Indeed, it is a stable glass of the Ge–Se system containing a high amount of selenium which is suitable for high nonlinear optical properties. The $\text{Ge}_{21}\text{Se}_{79}$ glass is then chosen as the clad composition. The clad glass has a T_g equal to $172 \text{ }^\circ\text{C} \pm 2 \text{ }^\circ\text{C}$ and an α equal to $270 \times 10^{-7} \text{K}^{-1} \pm 5 \times 10^{-7} \text{K}^{-1}$. The core has a T_g equal to $165 \text{ }^\circ\text{C} \pm 2 \text{ }^\circ\text{C}$ and α equal to $280 \times 10^{-7} \text{K}^{-1} \pm 5 \times 10^{-7} \text{K}^{-1}$. Thus for the clad glass the vitreous transition temperature T_g is 7 $^\circ\text{C}$ above these of the core glass and its expansion coefficient is $10 \times 10^{-7} \text{K}^{-1}$ lower than the core one.

The difference in the refractive indices between the clad glass and the core glass is equal to 2.4×10^{-3} at 1.55 μm . The numerical aperture calculated with Eq. (1) is equal to 0.10:

$$\text{N.A.} = \sqrt{n_c^2 - n_g^2} \quad (1)$$

The numerical aperture is related to the normalized frequency V defined by the following relation:

$$V = \frac{2\pi \cdot r}{\lambda} \text{N.A.} \quad (2)$$

where r is the core radius of the fiber and λ the signal wavelength. When $V < 2405$ [22], we have a single mode operation. According to Eq. (2), to have a single mode fiber at 1.55 μm in our conditions, the core diameter must be smaller than 12 μm .

3.2. Single mode optical fibers

3.2.1. Linear characterizations

From a preform with a diameter of 12 mm, 50 m of fiber with an external diameter of 280 μm have been drawn.

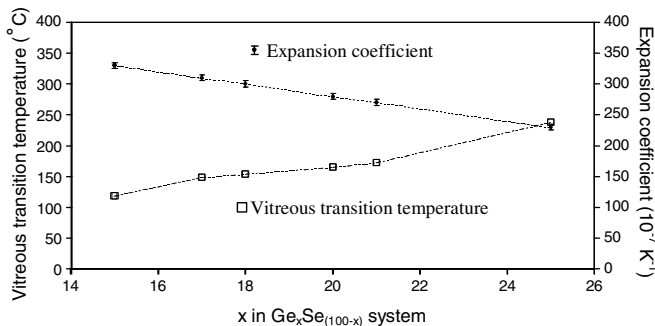


Fig. 3. Vitreous transition temperature T_g and expansion coefficient α of $\text{Ge}_x\text{Se}_{100-x}$ glass system.

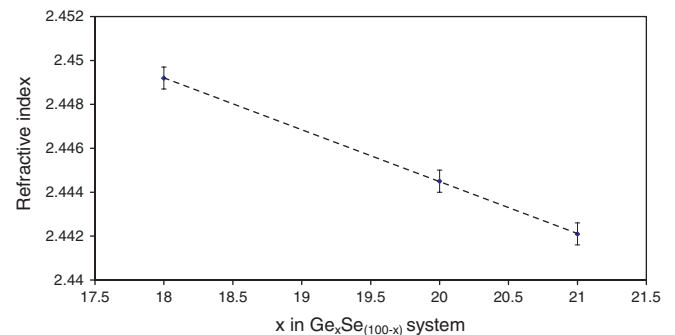


Fig. 4. Refractive indices of the $\text{Ge}_x\text{Se}_{100-x}$ glass system.

Fig. 5 shows a section of the fiber before the application of the vacuum at the core–clad interface. Fig. 6 illustrates the section of the fiber obtained with a vacuum of 100 mB. In the center of the fiber, we can see the round core which exhibits a diameter of 10 μm . No defect appears at the interface between the core and the clad.

In this fiber, we have measured an attenuation of 4 dB/m at 1.55 μm by the cut back method.

The guided mode injected with the laser fiber at 1.55 μm is observed in the near field (Fig. 7). The analysis of the beam proves the single mode character of the fiber. The Gaussian profile of the fundamental LP01 mode is shown in Fig. 8.

3.2.2. Nonlinear optical characterizations

The third order nonlinear coefficient n_2 of the fiber (Kerr coefficient) is measured through the spectral broadening of a high power picosecond pulse propagating in the fiber. The pulse profile creates, by means of the self phase modulation effect, a parabolic phase profile which enlarges the spectrum of the pulse. To determine the nonlinear Kerr coefficient, we have numerically studied the pulse propagation in the fiber, and we have adjusted the nonlinear coefficient so that the calculated spectrum fits with the experimental results. We solved the nonlinear Schrödinger equation for pulse propagation using the split-step Fourier

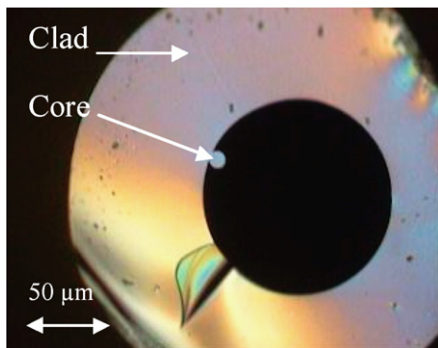


Fig. 5. Picture of section of the fiber observed with a light microscope before the application of the vacuum at the core–clad interface.

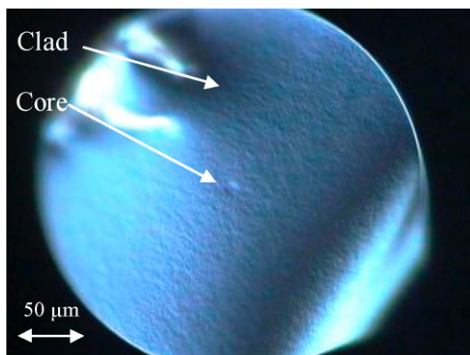


Fig. 6. Picture of section of the final fiber observed with a light microscope.

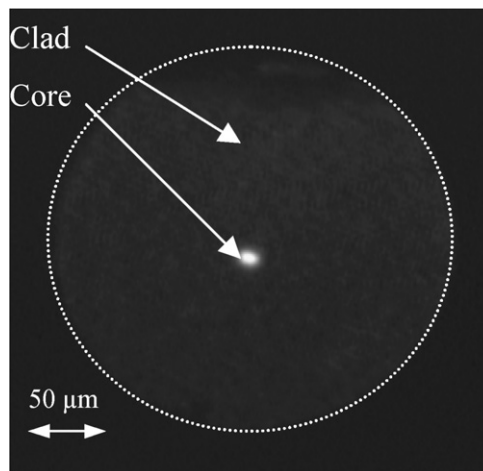


Fig. 7. Near field image at 1.55 μm of a GeSe₄ based optical fiber.

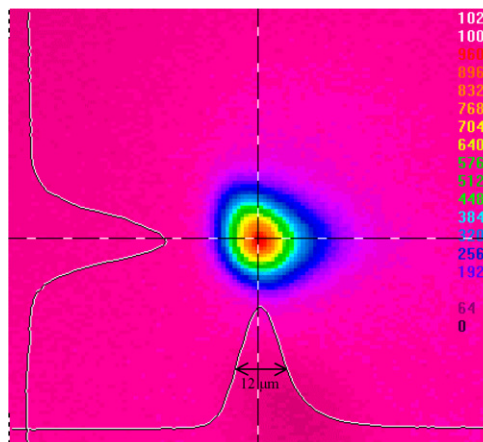


Fig. 8. Gaussian profile of the 1.55 μm guided beam in the GeSe₄ based optical fiber.

method [21]. The pulse duration is equal to 5 ps for our calculations and experiments, the spectral bandwidth is equal to 1.7 nm and the fiber length is 0.65 m. In these conditions, our calculations took no account of group velocity dispersion, high order dispersion and Brillouin effect. Moreover, the peak power is sufficiently weak to avoid Raman effect.

For our experiments, we use a single mode erbium fiber laser delivering optical pulses at 1545.7 nm with a repetition rate of 20 MHz. The pulse spectra are recorded using a spectrum analyzer. The temporal pulse profile is characterized with a noncollinear second harmonic generation based autocorrelator. The spectral broadening is measured at -20 dB versus the peak power of the input beam (Fig. 9). At low power (linear regime), the spectral broadening is not large enough to perform a reliable measurement. Then, the nonlinear coefficient has been determined for input powers ranging from 23.2 W to 55.0 W. For each input power, we calculate the nonlinear coefficient so that the calculated spectrum best fits with the measured one. In these conditions the n_2 value varies between $3.1 \times 10^{-18} \text{ m}^2/\text{W}$

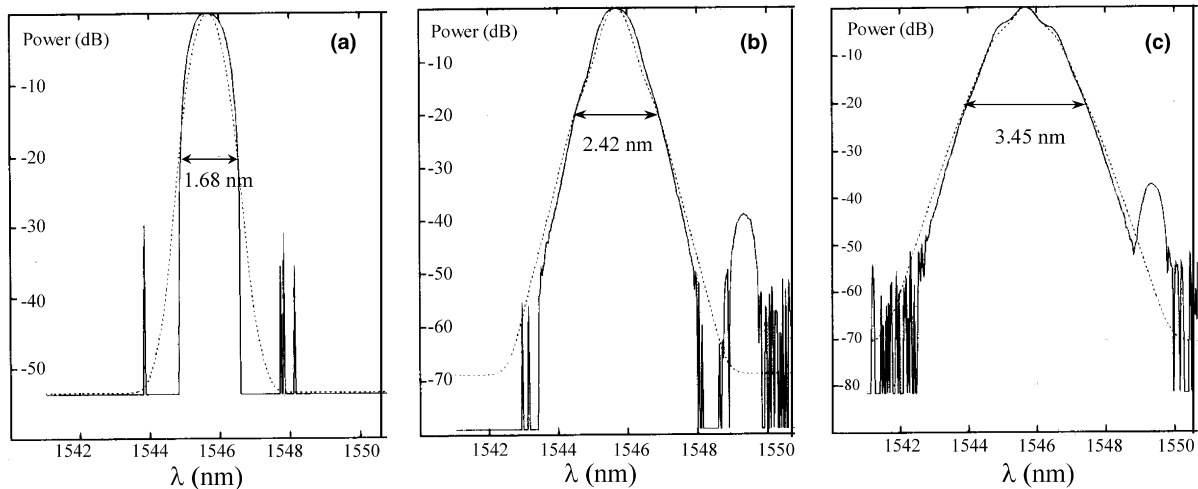


Fig. 9. Spectral broadening obtained for different input powers: (a) 109 mW, (b) 23,182 mW and (c) 55,045 mW.

Table 1
Spectral broadening ($\Delta\lambda$) and nonlinear coefficient (n_2) for different input powers (P_{in})

P_{in} (W)	$\Delta\lambda$ (nm)	n_2 (10^{-18} m ² /W)
23,182	2.42	3.2
28,969	2.60	3.1
34,774	2.78	3.2
40,560	3.03	3.3
46,365	3.24	3.3
55,045	3.45	3.1

and 3.2×10^{-18} m²/W, which proves the high reliability of the method (see Table 1).

4. Discussion

The $\text{Ge}_x\text{Se}_{100-x}$ vitreous system has been studied with x varying between 15 and 25. This system shows strong variations of the physical properties with the germanium rate. The vitreous transition temperature (T_g) and the expansion coefficient (α) are varying rapidly with a weak variation of the Ge content. As a consequence, it's necessary to choose rather close compositions to obtain a couple of glasses compatible with the single mode fiber elaboration. Indeed the difference between the T_g of the core and the clad glasses must be limited in order to reach the fibering viscosity for a similar temperature. This behavior is directly related to the nature of the vitreous network. Indeed, the germanium, which is 4-fold coordinated in a tetrahedral geometry, leads to a reticulated network, while the selenium, essentially 2-fold coordinated, is mainly in a two-dimensional geometry [23,24]. Thus an increase in the Ge content provokes immediately a higher reticulation of the network and an important increase of the vitreous transition temperature.

The values of the dilatation coefficients are also critical. Indeed, they must be close enough to avoid a mechanical stress in the fiber, which could lead to a mechanical fragility and to guiding defects.

Of course the refractive index of the core glass must be higher than that of the clad glass to allow the propagation of the beam in the core of the fiber.

On these basis, we have chosen the following couple of compositions: $\text{Ge}_{20}\text{Se}_{80}$ for the core and $\text{Ge}_{21}\text{Se}_{79}$ for the clad. These compositions present a T_g difference $\Delta T_g = 7$ °C, a dilatation coefficient difference of $\Delta\alpha = 10 \times 10^{-7}$ K⁻¹ and a refractive index difference of $\Delta n = 2.4 \times 10^{-3}$ at 1.55 μm . The numerical aperture of the fiber is then N.A. = 0.1. One can note that the two glasses are very close in composition and that the thermal parameters suitable for the drawing impose a small numerical aperture.

The improved method of single mode fiber elaboration named “fiber-in-tube” used in this work allows to obtain a single mode fiber with a reduced number of steps. The classical rod in tube method starting with a core rod of 4 mm in diameter would have required here more than five drawing steps of the initial preform to attend the single mode parameters. Thus, the elaboration is less time consuming. What's more the preform undergoes just one heating cycle for the fibering which is favorable to the vitreous quality. Indeed, successive heating cycles would be likely to initiate a crystallization not to be hoped. The utilization of a pressure control at the core–clad interface (i.e. a vacuum) allows also to reach a better collapse at this interface. The analysis of the beam profile at 1.55 μm (Fig. 8) confirms that the single mode operation has effectively been reached with this process.

The single mode fiber losses measured by cut back at 1.55 μm are around 4 dB/m. One can note that the minimum of attenuation that can be reached for an unclad core-only GeSe_4 fiber at 5.5 μm is 0.1 dB/m, with an attenuation around 0.8 dB/m at 1.55 μm [25]. This result is comparable to those obtained previously on unclad core-only GeSe_4 fibers [26,27]. The difference in losses between the unclad and the single mode fibers can be attributed to the purification process of the glasses which were further purified in the case of the unclad fibers. The large difference in

surface area between the core fiber and the inner surface of the cladding tube can also provoke a folding effect of the cladding tube around the core and can lead to scattering. In addition, the vacuum at the interface increases the volatilization of the selenium which can then deposit as soot at the core–clad interface in cooler regions, and thus increase again the scattering losses.

Concerning the nonlinear optical characterizations, different chalcogenide glass samples have been tested [7,9,11–17]. More particularly, for GeSe glasses, the determination of the nonlinear refractive index at 1.06 μm and 1.55 μm by different methods, the Z-scan technique [11–14], the Mach Zender interferometry [14–17] and the nonlinear imaging technique [16,17] has permit to qualify the nonlinear optical properties of this glass family. For the particular GeSe₄ glass, which is under interest in this work, the n_2 value is $n_2 = 15.6 \pm 2.5 \times 10^{-18} \text{ m}^2/\text{W}$ at 1.06 μm and $n_2 = 9 \pm 1.4 \times 10^{-18} \text{ m}^2/\text{W}$ at 1.55 μm from NIT measurements [16]. The nonlinear properties of GeSe₄ glass represent thus 400 times the nonlinearity of the silica glass ($n_2(\text{SiO}_2) = 2.2 \times 10^{-20} \text{ m}^2/\text{W}$ at 1.55 μm [21]).

In the case of the single mode fiber elaborated from GeSe₄ glass, the self phase modulation measurements have lead to a nonlinear refractive index of $3.3 \pm 1.5 \times 10^{-18} \text{ m}^2/\text{W}$ at 1.55 μm . This corresponds to 150 times the n_2 of SiO₂ glass. The difference observed with the values measured on the bulk glass can be explained by the fact that the technique of measurement is different. This variation is already observed in the bulk materials when different methods of measurement are used [14–17]. For example, the n_2 value of GeSe₄ measured by Z-scan at 1.06 μm is $13 \times 10^{-18} \text{ m}^2/\text{W}$ while the same glass measured by Mach Zender interferometry at the same wavelength (1.06 μm) leads to a value of $9 \times 10^{-18} \text{ m}^2/\text{W}$. One can expect that future improvements in the elaboration of selenide single mode fibers will lead to a level of attenuation close to that of the unclad core-only fibers. But, if we compare the figure of merit at 1.55 μm of selenide fibers and silica fibers, the selenide fibers level of losses remains unfavorable. However, the high infrared transparency of these fibers will allow to implement nonlinear effects in a wavelength range out of reach of silica fibers.

5. Conclusion

In this work, we have achieved an optical fiber, single mode at 1.55 μm , based on the GeSe₄ glass. The elaboration of the single mode fiber is performed by an improved method of drawing named “fiber-in-tube”. This method allows to realize a single mode fiber in only one drawing step after the elaboration of the core/clad “fiber-in-tube” preform. The optical losses of this fiber are 4 dB/m at 1.55 μm . The self phase modulation measurements have

lead to a nonlinear refractive index of $3.3 \times 10^{-18} \text{ m}^2/\text{W}$ at 1.55 μm which corresponds to 150 times the nonlinearity of silica glass.

References

- [1] L.B. Shaw, P.C. Pureza, V.Q. Nguyen, J.S. Sanghera, I.D. Aggarwal, P.A. Thielen, Trends in Optics and Photonics Advanced Solid-State Lasers, vol. 68, 2002, p. 19.
- [2] P.A. Thielen, L.B. Shaw, P.C. Pureza, V.Q. Nguyen, J.S. Sanghera, I.D. Aggarwal, Opt. Lett. 28 (16) (2003) 1406.
- [3] S. Savage, J. Shelby, B.S. Robinson, S.A. Hamilton, E.P. Ippen, Opt. Lett. 28 (1) (2003) 13.
- [4] N. Sugimoto, J. Am. Ceram. Soc. 85 (5) (2002) 1083.
- [5] Y. Seungwoo, K.M. Yoon, Y.G. Lee, E. Jinseob, Jpn. J. Appl. Phys. 2B (2004) 43.
- [6] K. Ogusu, J. Yamasaki, S. Maeda, M. Kitao, M. Minakata, Opt. Lett. 29 (3) (2004) 265.
- [7] J.M. Harbold, F.O. Ilday, F.W. Wise, J.S. Sanghera, V.Q. Nguyen, L.B. Shaw, I.D. Aggarwal, Opt. Lett. 27 (2) (2002) 119.
- [8] S. Smolorz, I. Kang, F. Wise, B.G. Aitken, N.F. Borrelli, J. Non-Cryst. Solids 256–257 (1999) 310.
- [9] J.M. Harbold, F.O. Ilday, F.W. Wise, B.G. Aitken, IEEE Photon. Technol. Lett. 14 (6) (2002) 822.
- [10] J.S. Sanghera, I.D. Aggarwal, L.E. Busse, P.C. Pureza, V.Q. Nguyen, L.B. Shaw, F.H. Kun, F. Chenard, Laser Focus World (April) (2005).
- [11] F. Smektala, C. Quémard, L. LeNeindre, J. Lucas, A. Barthélémy, C. De Angelis, J. Non-Cryst. Solids 239 (1998) 139.
- [12] C. Quémard, F. Smektala, V. Couderc, A. Barthélémy, J. Lucas, J. Phys. Chem. Solids 62 (2001) 1435.
- [13] F. Smektala, C. Quémard, V. Couderc, A. Barthélémy, J. Non-Cryst. Solids 274 (2000) 232.
- [14] G. Boudebs, F. Sanchez, J. Troles, F. Smektala, Opt. Commun. 199 (2001) 425.
- [15] F. Smektala, J. Troles, V. Couderc, A. Barthélémy, G. Boudebs, F. Sanchez, H. Zeglache, G. Martinelli, Y. Quiquempois, P. Bernage, SPIE 4628 (2002) 30.
- [16] F. Smektala, J. Troles, P. Houizot, T. Jouan, G. Boudebs, S. Cherukulappurath, V. Couderc, P.A. Champert, SPIE 5451 (2004) 347.
- [17] A. Monteil, G. Boudebs, F. Sanchez, C. Duverger, B. Boulard, J. Troles, F. Smektala, SPIE 4829 (2004) 109.
- [18] P.W. France, M.G. Drexhage, J.M. Parker, M.W. Moore, S.F. Carter, J.V. Wright, Fluoride Glass Optical Fibers, Blackie, Glasgow and London, 1990.
- [19] D.C. Tran, C.F. Fisher, G.H. Sigel, Elect. Lett. 18 (1982) 657.
- [20] R.D. Driver, G.M. Leskowitz, L.E. Curtiss, D.E. Moynihan, L.B. Vacha, Mater. Res. Soc. Symp. Proc. 172 (1990) 169.
- [21] G.P. Agrawal, Nonlinear Fiber Optics, third ed., Academic Press, 2001 (Chapter 4).
- [22] C. Yeh, Handbook of Fiber Optics, Academic Press, Inc., San Diego, 1990.
- [23] B. Bureau, J. Troles, M. Le Floch, P. Guénot, F. Smektala, J. Lucas, J. Non-Cryst. Solids 319 (1–2) (2003) 145.
- [24] B. Bureau, J. Troles, M. Le Floch, F. Smektala, J. Lucas, J. Non-Cryst. Solids 326–327 (2003) 58.
- [25] P. Houizot, Ph.D. Thesis of University of Rennes, France, 2004.
- [26] T. Kanamori, Y. Terunuma, S. Takahashi, T. Miyashita, J. Light-wave Technol. LT-2 (1984) 607.
- [27] T. Katsuyama, S. Satoh, H. Matsumura, J. Appl. Phys. 71 (1992) 4132.